

Title	Vortex dynamics in anisotropic traps
Authors	McEndoo, Suzanne; Busch, Thomas
Publication date	2010
Original Citation	McEndoo, S. and Busch, T. (2010) 'Vortex dynamics in anisotropic traps', Physical Review A, 82(1), pp. 013628. (5pp). doi: 10.1103/PhysRevA.82.013628
Type of publication	Article (peer-reviewed)
Link to publisher's version	https://journals.aps.org/pr/abstract/10.1103/PhysRevA.82.013628 - 10.1103/PhysRevA.82.013628
Rights	© 2010, American Physical Society
Download date	2023-05-07 22:04:37
Item downloaded from	http://hdl.handle.net/10468/4528

Vortex dynamics in anisotropic traps

S. McEndoo and Th. Busch

Department of Physics, University College Cork, Cork, Ireland

(Received 7 May 2010; published 21 July 2010)

We investigate the dynamics of linear vortex lattices in anisotropic traps in two dimensions and show that the interplay between the rotation and the anisotropy leads to a rich but highly regular dynamics.

DOI: [10.1103/PhysRevA.82.013628](https://doi.org/10.1103/PhysRevA.82.013628)

PACS number(s): 03.75.Kk, 67.85.De

I. INTRODUCTION

Since their first observation in solid-state superconductors [1] and liquid ^4He [2], arrays of quantized vortices have been one of the key features of systems that exhibit frictionless flow. More recently, the observation of vortex lattices in gaseous Bose-Einstein condensates [3,4] has led to a renewed interest in these systems, as ultracold atomic gases are highly configurable systems and allow for investigation of the lattices under a wide range of external parameters. Since then, a large number of theoretical and experimental studies have been undertaken, which, for example, have examined the equilibrium properties of vortex lattices in different external potentials [5,6] or the dynamical properties of vortex lattices when disturbed [7]. At the same time, new ideas for applications in quantum information [8,9] and precision measurement [10] have been developed.

The geometry of a vortex lattice is determined by the condition to minimize the energy of the overall system under the provision of fixed angular momentum. It, therefore, depends on the interaction energy between the velocity fields of the vortices, which is a logarithmic function of the distance between, and the underlying external potential. For Bose-Einstein condensates that carry large angular momentum in isotropic harmonic traps, this leads to the formation of triangular Abrikosov lattices of vortices with winding number 1 [4,11]. For trap geometries that are not simply connected, such as toroidal shapes, the system can also respond by forming persistent currents with higher winding numbers [12]. Other trap geometries and parameters, such as anisotropic traps [13–15] or optical lattices [5], no longer support an Abrikosov lattice, but instead form zigzag or linear and square lattices, respectively.

While vortices and vortex lattices are interesting to study on their own merits [16,17], it has been suggested that they can be used in quantum information applications by the encoding of information into the winding number [8,9]. These numbers are so-called geometrical quantum numbers, which have the advantage of not suffering from any energetic instabilities and which are stable as long as the vortex cores are part of the system. Transferring the atoms into superposition states of these quantum numbers can be done either by optical methods [8], or by making use of anisotropic external potentials [18]. However, due to the very dense energy spectrum of atomic superfluid systems, it is a very difficult task to separate out exactly two flow states [19,20]. Since the vortex-vortex interaction is dependent on both magnitude and direction of rotation, however, one can, in principle, imagine a setup for a superfluid quantum computer analogous to the linear ion-trap model of Cirac and Zoller [21]. In order to facilitate control and

to address the individual vortex qubits, it, therefore, would be preferable to reduce the number of nearest neighbors from six, in the Abrikosov lattice, to, say, two in a linear crystal. Today, it is known that two systems with which this can be achieved are waveguides [14,22] and anisotropic traps [13,15].

Here, we consider the latter systems at medium rotation and with small numbers of vortices. For currently typical experimental nonlinearities, it was recently found that even relatively small anisotropies $\lambda \approx 2$ lead to the vortices that form linear crystals with equal spacing between them [15,23]. However, the inhomogeneity of the background gas leads to a finite velocity of the vortex lattice within the cloud [24], which, in the limit of large vorticity, cancels out the external rotation [4]. For systems of medium vorticity in an anisotropic trap, it is obvious that the linear shape of the crystal cannot be maintained during these dynamics; and, here, we will show that this results in excitations within the background cloud, which can be described by a standard hydrodynamics approach [25,26]. More surprisingly, we also find that the excitations are oscillatory and do not destroy the ordering of the vortex lattice, even in the situation when the external rotation is switched off.

In the following, we will first briefly introduce our model and then examine the dynamics of the linear vortex lattices as a function of anisotropy by integrating the underlying Gross-Pitaevskii equation for time scales of several hundred milliseconds. We determine the characteristic excitation frequencies of the vortex lattice and compare them to the known frequencies for anisotropic condensates. Finally, we remark on the stability of the vortices themselves.

II. ANISOTROPIC TRAPPING POTENTIALS

To simulate the dynamics of the vortices, we consider a two-dimensional model of Bose condensed gas of particles of mass m in a harmonic trap $V_{\text{HO}} = \frac{1}{2}m(\omega_x^2 x^2 + \omega_y^2 y^2)$, where the anisotropy is determined by the aspect ratio $\lambda = \omega_y/\omega_x$. The trap is rotating around the z axis, and we assume that a strong potential suppresses all relevant dynamics in this direction. For small, but nonnegligible anisotropies ($\lambda \gtrsim 2$ for typical experimental systems), the ground state for medium rotation frequencies is given by a single line of vortices along the weak axis of the trap [15]. In the case of an odd number of vortices, one vortex will be located at the center of the trap, and the others will be symmetrically arranged around it. For an even number, the same symmetry exists, however, without the central vortex. Furthermore, the vortex spacing remains roughly even along the soft axis due to the slow variation of the condensate density.

For large rotational frequencies, the condensate's efforts to distribute the vorticity as uniformly as possible lead to a self-consistent solid-body rotation, which cancels out the overall rotations of the lattice in the corotating frame [24]. In the region of medium vorticity, however, in which only a few vortices are present, the concept of a diffused vorticity cannot be applied, and the vortex lattice will try to carry out rotation in the comoving frame. It is not surprising that, in anisotropic traps, this will lead to a dynamics that will have a feedback onto the density distribution of the atomic cloud.

In the following, we will consider these dynamics as a function of the trap anisotropy for the case of ^{87}Rb and currently realistic trapping frequencies. All our simulations are done by numerically integrating the Gross-Pitaevskii equation by using a fast Fourier transform or split-operator method.

III. DYNAMICS AS FUNCTION OF ANISOTROPY

The Hamiltonian for a Bose-Einstein condensate in an anisotropic trap and under rotation is given by

$$H = -\frac{\hbar^2}{2m}\nabla^2 + V_{\text{HO}} - \Omega L_z + \frac{gN}{2}|\psi|^2, \quad (1)$$

where N is the number of atoms and Ω is the frequency with which the trap rotates around the z axis. As usual, for stability reasons, Ω is restricted to values smaller than the trapping frequency of the soft axis of the condensate. The two-dimensional interaction strength is given by $g = (4\pi\hbar^2 a_{sc}/m)(m\omega_z/2\pi\hbar)^{1/2}$, with $a_{sc} = 4.67$ nm as the three-dimensional scattering length for ^{87}Rb in the $|2, 1\rangle$ state.

We are interested in studying the behavior of a ground-state lattice as a function of time. While the behavior of the condensate as a whole can be studied by using a hydrodynamics approach in the Thomas-Fermi limit [25,26], the dynamics of the vortices themselves require an approach that is able to resolve the dynamics on the length scale of the healing length, such as the Gross-Pitaevskii equation. To have a clean initial state, we, therefore, first find the ground state of the Hamiltonian of Eq. (1) by a numerical relaxation method and then integrate this state in time while maintaining the rotation.

The results of the numerical integration for a crystal of five vortices in a trap of aspect ratio $\lambda = 2.5$ are shown in Fig. 1. The upper half shows the starting configuration, and the lower half displays the positions of the individual vortices as a function of time along the soft direction of the trap. The detailed displacement in the tight direction of the trap is shown in Fig. 2, and its range is indicated by the dashed lines in Fig. 1. There are four immediate observations one can make from looking at these results: (i) The trajectories in both directions are symmetric for the pairs of vortices that are at equal distance from the center of the trap. The central vortex remains stationary at all times; (ii) while the oscillation amplitudes for the two inner and the two outer vortices are different, they are in phase with each other during the whole evolution; (iii) the vortex motion is periodic, and, in particular, the direction of rotation of the lattice reverses regularly; and (iv) the paths of the vortices never cross, and the linear ordering is maintained at all times. Closer examination shows that the trajectories of the two vortices on the right-hand side and the two vortices on the left-hand side follow the exact

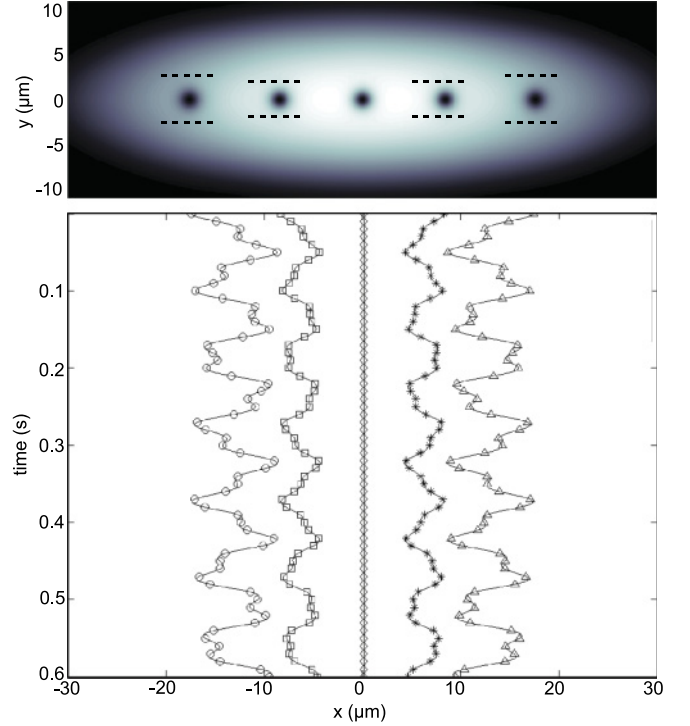


FIG. 1. (Color online) The ground-state density for a condensate of $N = 10^5$ Rb atoms in a trap with $\lambda = 2.5$ and $\omega_x = 10 \times 2\pi$ Hz (upper panel) and the oscillatory trajectories of the vortices along the x axis as a function of time (lower panel). The center vortex can be seen to remain stationary, while the other four vortices periodically oscillate away from their initial position. The dashed lines in the density plot indicate the range of movement in the y direction for each of the vortices (see Fig. 2).

same pattern and are only different by a constant factor in their amplitude. This applies to the motion in the x as well as in the y direction and shows that the distance between neighboring pairs of vortices is the same at any point in time. We have calculated these dynamics for different aspect ratios and consistently found the behavior. As an example, Fig. 3 shows the results for a trap with an aspect ratio of $\lambda = 3.5$, for which the same behavior, apart from a smaller amplitude of the oscillations, is found.

To better understand this pattern, in Table I, we show the dominating oscillation frequencies for the vortex oscillations in three different traps. For all anisotropies, we find two dominating frequencies ω_1 and ω_2 , and in the soft direction, the lower frequency has a larger amplitude, whereas in the tight direction, the opposite is true. For increasing anisotropy, the lower frequency decreases, whereas the higher frequency increases. This can clearly not be explained by straightforward oscillations in the harmonic potential, but indicates that the nonlinearity of the sample plays a significant role. At the same time, it is also clear that the oscillation does not originate from a simply stationary vortex crystal inside an oscillating background cloud, as the cloud would be stationary in the corotating frame. However, we will show in the following that both factors are playing an important role.

Let us describe the dynamics of the background cloud by using a hydrodynamic formalism and assume that the

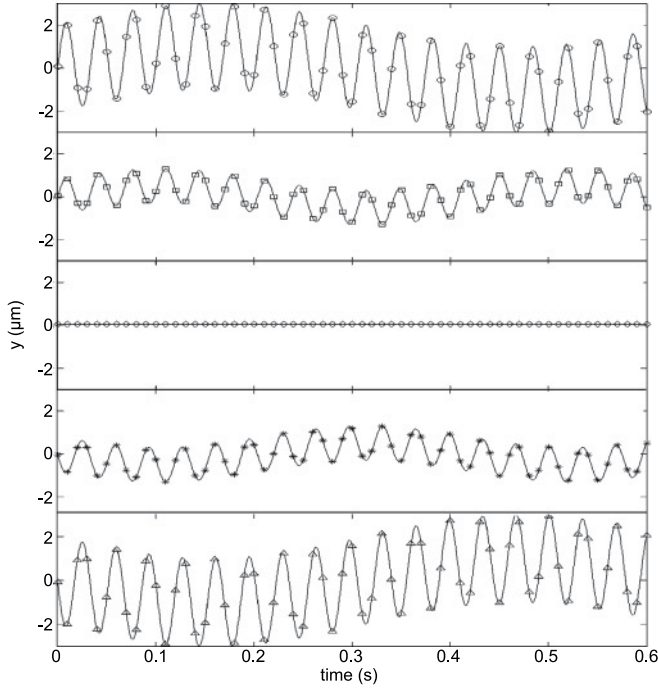


FIG. 2. The position of the vortices in the y direction, which corresponds to the situation shown in Fig. 1. The top row shows the leftmost vortex, and the bottom row shows the rightmost one.

excitation of it is triggered and is driven by the motion of the vortices. In fact, we assume that the rotation of the vortices leads to an infinitesimal rotation of the whole cloud, and we solve the classical hydrodynamical equations from there. This scenario was recently investigated by Lobo and Castin in order to find the scissors mode of a rotating condensate with vortices [26].

The density profile $\rho(\mathbf{r})$ and the velocity field $\mathbf{v}(\mathbf{r})$ of a condensate in a rotating anisotropic trap in the Thomas-Fermi limit in the corotating frame can be described by the equations of classical hydrodynamics as

$$(\partial_t + \mathbf{v} \cdot \nabla) \mathbf{v} = -\frac{1}{m} \nabla(U + \rho g) - 2\boldsymbol{\Omega} \times \mathbf{v} - \boldsymbol{\Omega} \times (\boldsymbol{\Omega} \times \mathbf{r}), \quad (2)$$

$$\partial_t \rho + \nabla \cdot \rho \mathbf{v} = 0. \quad (3)$$

Because we have chosen the ground state with a stationary linear vortex lattice as the initial condition for the cloud, the condensate is characterized by $\mathbf{v} \approx \mathbf{0}$ for the velocity field and by the Thomas-Fermi solution for the density:

$$\rho_0(x, y) = \frac{m}{2g} [2\mu - (\omega_x^2 - \Omega^2)x^2 - (\omega_y^2 - \Omega^2)y^2]. \quad (4)$$

We assume that the rotation of the vortex lattice, and, therefore, the change in the associated flow, leads to a small initial disturbance that corresponds to a rotation of the whole system with respect to the trap. It can be described by a small angle θ , from which the initial conditions for the linear perturbations to the preceding equations are given as $\delta \mathbf{v} = \mathbf{0}$ and $\delta \rho = \theta m x y (\omega_x^2 - \omega_y^2)/g$ [26]. The subsequent dynamical

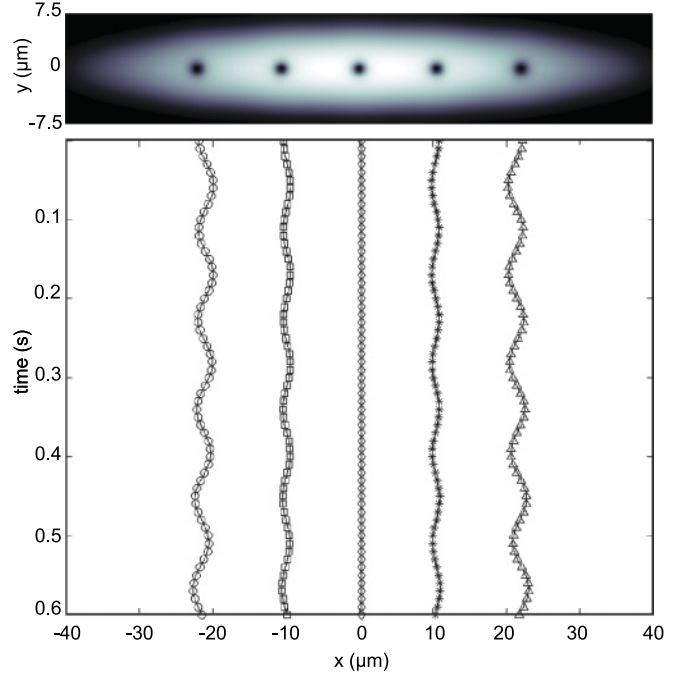


FIG. 3. (Color online) The ground-state density for $\lambda = 3.5$ (upper panel and the position of the vortices along the x axis (lower panel). All system parameters are the same as in the $\lambda = 2.5$ case, and all observations made apply here as well with reduced amplitude. In the y direction, the movement is on the order of 1×10^{-7} m (not shown).

evolution can then be calculated by using the time-dependent polynomial ansatz,

$$\delta \rho = \frac{m}{g} [c(t) - \mathbf{r} \cdot \delta A(t) \mathbf{r}], \quad (5)$$

$$\delta \mathbf{v} = \delta B(t) \mathbf{r}, \quad (6)$$

where $\delta A(t)$ is a symmetric and $\delta B(t)$ is a general 2×2 matrix, and the chemical potential enters via the evolution of the number $c(t)$ [26]. The numerical solution of these equations shows an oscillation pattern, which again is dominated by two main frequencies ω_{h1} and ω_{h2} , and which we have tabulated in Table I.

While these are not, and were not expected to be, a perfect match for the lattice oscillation frequencies, they are closer in value and, in particular, show the same trend of increase and decrease. This shows that the oscillations of the lattice excite and drive oscillations within the background cloud, which,

TABLE I. Frequencies dominating the oscillation of the vortex lattice from the numerical integration of the Gross-Pitaevskii equation (ω_1 and ω_2) and oscillation frequencies from the hydrodynamic model for the background cloud (ω_{h1} and ω_{h2}) for different values of the anisotropy. For comparison, the trapping frequencies are shown as well.

λ	ω_x (Hz)	ω_y (Hz)	ω_1 (Hz)	ω_2 (Hz)	ω_{h1} (Hz)	ω_{h2} (Hz)
2.5	62.8	157.1	69.0	187.9	69	182
3.0	62.8	188.5	60.0	210.0	67	210
3.5	62.8	219.9	53.7	254.4	62	239

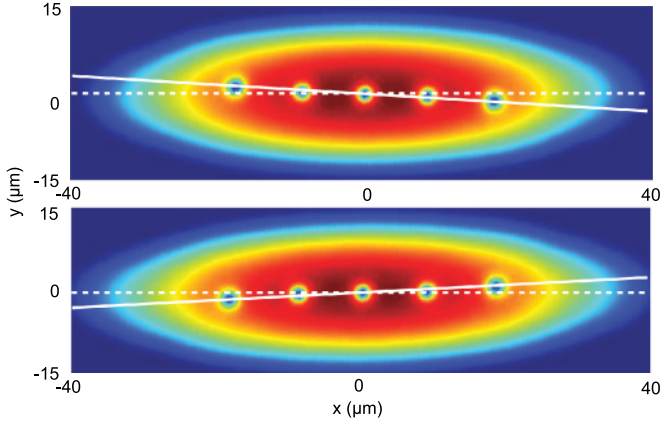


FIG. 4. (Color online) Density of the cloud at $t = 0.0072$ s (upper panel) and $t = 0.0108$ s (lower panel). The full white line indicates the tilted axis of the vortex crystal, and the broken white line indicates the horizontal starting position. The oscillation of amplitude of the background cloud is too small to be visible in this plot.

in turn, feeds back onto the lattice dynamics to create the continuous and periodic behavior. This is also demonstrated by the fact that the amplitude of the lattice oscillations is significantly larger than the amplitudes of the cloud. In Fig. 4, we show that the oscillation angle of the lattice cloud is clearly much larger than the one for the background cloud, which, in fact, stays very close to its initial distribution. Nevertheless, the whole dynamics is highly predictable, and, in particular, the order of the vortices is maintained throughout.

IV. DYNAMICS IN THE ABSENCE OF ROTATION

It is interesting to investigate the robustness of the order of the vortex lattice under even stronger perturbations of the background cloud, and we will, therefore, in the following, investigate the dynamics of the cloud in the absence of external rotation. From the previous results, it should be clear that the background flow will be strongly disturbed by the now nonrotating trapping potential, and one might expect the linear vortex crystal to break up into a random pattern. Although, as the system is finite, it is clear that after some evolution, the linear form has to be reassumed.

In Fig. 5, we show an example of the time evolution of a cloud initially with five vortices aligned along the soft axis (a) and an aspect ratio of $\lambda = 2.5$. The vortex crystal can be seen to rotate against the cloud, still maintaining its linear shape after $t = 0.03$ s (b). After a further 0.03 s, the linear geometry is slightly disturbed when the vortices are passing through the narrow direction of the condensate (c), but they finally assume the linear shape again after about 0.1 s (d). As for the case of maintained trap rotation, the outermost pair of vortices follows a symmetrical path, as do the inner pair of vortices. However, once the narrow section is passed, the pairs on each side have changed their order for the first time (see Fig. 6), and this process will be repeated over and over again during the ensuing evolution. The vortices also regularly form a linear crystal again [see Fig. 6(d)], however, not necessarily along the horizontal axis. This behavior persists for higher ratios of the anisotropy, until the condensate itself decays too

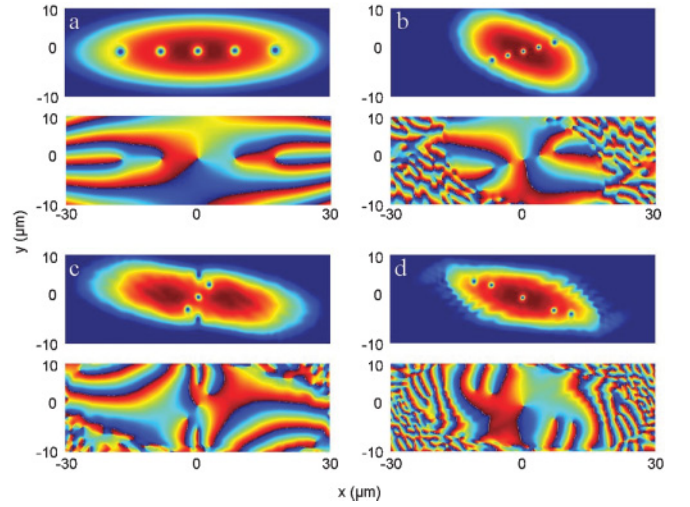


FIG. 5. (Color online) Dynamical evolution of the density and phase for a trap of aspect ratio $\lambda = 2.5$ for which the rotation has been switched off. Panel (a) shows the initial linear crystal at $t = 0$ s, and the subsequent panels show the times (b) $t = 0.03$ s, (c) $t = 0.06$ s, and (d) $t = 0.1$ s. Panel (c) shows the disturbed crystal as outer vortices pass the narrow direction of the condensate as they rotate around the central vortex, and panel (d) shows the reformation of the linear crystal. At this time, the left and right pairs of vortices have rotated around the central vortex, and the inner and outer vortices on each side have swapped positions. The phase plots show that the charge of the vortices is maintained throughout the time evolution.

fast, due to the anisotropic barrier it runs into, to be able to define a clear vortex crystal.

V. STABILITY OF VORTICES

Finally, let us briefly comment on the stability of vortices in the lattice. As the systems we investigate are not rotationally

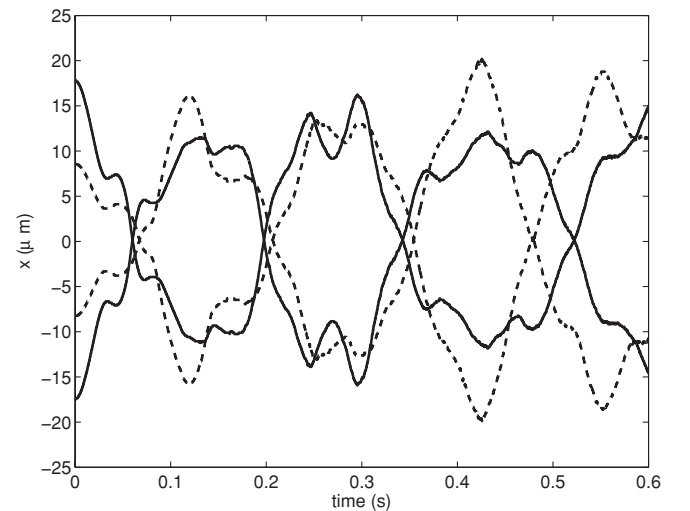


FIG. 6. Position of the vortices along the x direction for $\Omega = 0$ and for $\lambda = 2.5$. The values for the initially outer pair of vortices are given by the full line, and the values for the inner pair of vortices are given by the broken line. It can be seen that the paths remain symmetrical for the respective pairs, however, they switch positions periodically.

symmetric, they do not need to conserve angular momentum, and it is possible for the vortices to reverse their direction of flow [27,28]. However, this tunneling between different rotational states is suppressed at larger interaction strengths, and as all our simulations are carried out in the Thomas-Fermi limit, we have checked that all vortices keep their initial rotational direction throughout the simulations. To demonstrate this for one example, we show the phase distributions for the case of the nonrotating cloud in Fig. 6.

VI. CONCLUSION

We have numerically investigated the dynamics of a linear vortex lattice in an anisotropic two-dimensional Bose-Einstein condensate. Starting from the ground state of the Gross-Pitaevskii equation, we have found that the vortices retain an ordered structure both in the presence and in the absence of rotation for time scales on the order of 1 s. If the

rotation of the cloud is maintained, the vortex lattice remains linear and only carries out well-defined oscillations within the background cloud. With increased anisotropy, oscillation amplitude decreases until, finally, the crystal does not move within the cloud. This allows for the use of the vortex lattices in applications such as, for example, quantum information. In the absence of rotation, we found that the outer vortices circle around the central vortex, periodically reversing their order, and the lattice and linear crystals are periodically reformed for anisotropies that are not too large. Once these get too strong, the background cloud gets too distorted to still talk about a well-defined vortex lattice.

ACKNOWLEDGMENT

The work was supported by Science Foundation Ireland under Project Number 05/IN/I852.

-
- [1] U. Essmann and H. Träuble, *Phys. Lett. A* **24**, 526 (1967).
 - [2] E. J. Yarmchuk, M. J. V. Gordon, and R. E. Packard, *Phys. Rev. Lett.* **43**, 214 (1979).
 - [3] K. W. Madison, F. Chevy, W. Wohlleben, and J. Dalibard, *J. Mod. Opt.* **47**, 2715 (2000).
 - [4] J. R. Abo-Shaeer, C. Raman, J. M. Vogels, and W. Ketterle, *Science* **292**, 476 (2001).
 - [5] J. W. Reijnders and R. A. Duine, *Phys. Rev. Lett.* **93**, 060401 (2004).
 - [6] A. Aftalion and I. Danaila, *Phys. Rev. A* **69**, 033608 (2004).
 - [7] I. Coddington, P. Engels, V. Schweikhard, and E. A. Cornell, *Phys. Rev. Lett.* **91**, 100402 (2003).
 - [8] K. T. Kapale and J. P. Dowling, *Phys. Rev. Lett.* **95**, 173601 (2005).
 - [9] S. Thanvanthri, K. T. Kapale, and J. P. Dowling, *Phys. Rev. A* **77**, 053825 (2008).
 - [10] S. Thanvanthri, K. T. Kapale, and J. P. Dowling, e-print [arXiv:0907.1138](https://arxiv.org/abs/0907.1138).
 - [11] J. R. Anglin and M. Caccioppo, e-print [arXiv:cond-mat/0210063v1](https://arxiv.org/abs/cond-mat/0210063v1).
 - [12] C. Ryu, M. F. Andersen, P. Cladé, V. Natarajan, K. Helmerson, and W. D. Phillips, *Phys. Rev. Lett.* **99**, 260401 (2007).
 - [13] M. Ö. Oktel, *Phys. Rev. A* **69**, 023618 (2004).
 - [14] S. Sinha and G. V. Shlyapnikov, *Phys. Rev. Lett.* **94**, 150401 (2005).
 - [15] S. McEndoo and T. Busch, *Phys. Rev. A* **79**, 053616 (2009).
 - [16] A. L. Fetter and A. A. Svidzinsky, *J. Phys. Condens. Matter* **13**, R135 (2001).
 - [17] A. L. Fetter, *Rev. Mod. Phys.* **81**, 647 (2009).
 - [18] V. M. Pérez-García, M. A. García-March, and A. Ferrando, *Phys. Rev. A* **75**, 033618 (2007).
 - [19] D. W. Hallwood, K. Burnett, and J. Dunningham, *J. Mod. Opt.* **54**, 2129 (2007).
 - [20] A. Nunnenkamp, A. M. Rey, and K. Burnett, *Phys. Rev. A* **77**, 023622 (2008).
 - [21] J. I. Cirac and P. Zoller, *Phys. Rev. Lett.* **74**, 4091 (1995).
 - [22] P. Sánchez-Lotero and J. J. Palacios, *Phys. Rev. A* **72**, 043613 (2005).
 - [23] N. Lo Gullo, T. Busch, and M. Paternostro (to be published).
 - [24] R. P. Feynman, in *Progress in Low Temperature Physics*, edited by C. J. Gorter (North-Holland, Amsterdam, 1955), Vol. 1, p. 17.
 - [25] M. Cozzini, S. Stringari, V. Bretin, P. Rosenbusch, and J. Dalibard, *Phys. Rev. A* **67**, 021602(R) (2003).
 - [26] C. Lobo and Y. Castin, *Phys. Rev. A* **72**, 043606 (2005).
 - [27] J. J. García-Ripoll, G. Molina-Terriza, V. M. Pérez-García, and L. Torner, *Phys. Rev. Lett.* **87**, 140403 (2001).
 - [28] G. Watanabe and C. J. Pethick, *Phys. Rev. A* **76**, 021605(R) (2007).